III. EFFECT OF A PRIOR STRETCH ON THE AGING RESPONSE OF AN Al-Cu-Li-Ag-Mg-Zr ALLOY

K.S. Kumar, S.A. Brown, and J.R. Pickens

1. INTRODUCTION

Recently, a family of Al-Cu-Li alloys containing minor amounts of Ag, Mg, and Zr and having desirable combinations of strength and toughness has been developed (1). These "Weldalite™" alloys exhibit a unique characteristic in that with or without a prior stretch, they obtain significant strength-ductility combinations upon natural and artificial aging. The ultra-high strength (~690 MPa yield strength) in the peak-aged tempers (T6, T8) has been primarily attributed to the extremely fine T_1 (Al_2CuLi) or T_1-type precipitates that occur in these alloys during artificial aging (2), whereas the significant natural aging response observed is attributed to strengthening from δ' (Al_3Li) and GP zones. (3) In recent work (4), the aging behavior of an Al-Cu-Li-Ag-Mg alloy without a prior stretch was followed microstructurally from the T4 to the T6 condition. Commercial extrusions, rolled plates, and sheets of Al-Cu-Li alloys are typically subjected to a stretching operation before artificial aging to straighten the extrusions and, more importantly, introduce dislocations to stimulate precipitation of strengthening phases such as T_1 by providing relatively low-energy nucleation sites (5,6).

The goals of this study are to examine the microstructure that evolves during aging of an alloy that was stretched after solution treatment and to compare the observations with those in sections I and II of this report for the unstretched alloy.

2. EXPERIMENTAL PROCEDURE

An extruded section of an aluminum alloy containing 5.3Cu-1.4Li-0.4Ag-0.4Mg-0.17Zr (wt%) and incorporating a 3% stretch was artificially aged at 160°C (433K) in a circulating air furnace. Prior to stretching, the extrusions were solutionized at 504°C (777K) for 1 h and water quenched to room temperature. The quenched and stretched material was allowed to age naturally at room temperature for >1000 hours to obtain the T3 condition.

The aging response was monitored using Rockwell B hardness measurements and select specimens along the aging curve [T3, T4 (without stretch), T4 + 15 min, T3 + 15 min, T3 + 2 h, T3 + 4 h, T3 + 20 h, and T3 + 100 h] were examined using transmission electron microscopy (TEM). Since the unstretched material in the previous

study (4) was aged at 180°C (453K), the stretched material in this study was also examined after exposure at 180°C (453K) for 15 min to allow a direct comparison with the unstretched material as well as the stretched material exposed to 160°C (433K) for the same time.

Specimens to be analyzed by TEM were sliced from the extrusions and mechanically ground to the desired thickness. These were then twin jet electropolished to perforation at 243K and 12 - 15 volts in a solution of 25% HNO_3 in methanol. After polishing, the specimens were dipped in a solution of 50% HNO_3 in H_2O to remove any Ag which may have redeposited from the electrolyte. Selected area diffraction (SAD) and centered dark field imaging (CDF) were used to follow the microstructural evolution during aging. Due to space limitations, in most cases only SAD patterns are provided, although CDF was used in each instance to confirm SAD observations.

3. RESULTS

The change in hardness with aging time at temperature is shown in Fig. 1 for both, the stretched and unstretched material. As mentioned earlier, the stretched material was aged at 160°C (433K), whereas the unstretched material was aged at 180°C (453K).* Several interesting features are present in Fig. 1 including a higher hardness for the T4 than the T3 condition and a reversion for the T3 and T4 conditions upon artificial aging for ~15 - 45 minutes, although the loss in hardness is more dramatic for the T4 condition. Subsequent artificial aging leads to equivalent peak hardness for both the stretched (T3) and unstretched (T4) material, although the T4 material ages faster than the T3 material at the temperatures investigated. In both cases, a very high peak hardness (T6 or T8) of ~95 - 97 R_B is reached. A sample of the unstretched material was also aged for 15 min at 160°C (433K) to provide a direct comparison of the reversion behavior with that of the stretched material. In this case, the hardness was found to be intermediate between that of T4 + 15 min at 180°C (453K) and T3 + 15 min at 160°C (433K).

---

* [Strictly speaking, the T3 and T4 conditions, which are naturally aged conditions, cannot be plotted in Fig. 1; however, for the purpose of providing a reference, they have been plotted on the hardness axis (T3 and T4 should actually reflect zero time at temperature)].

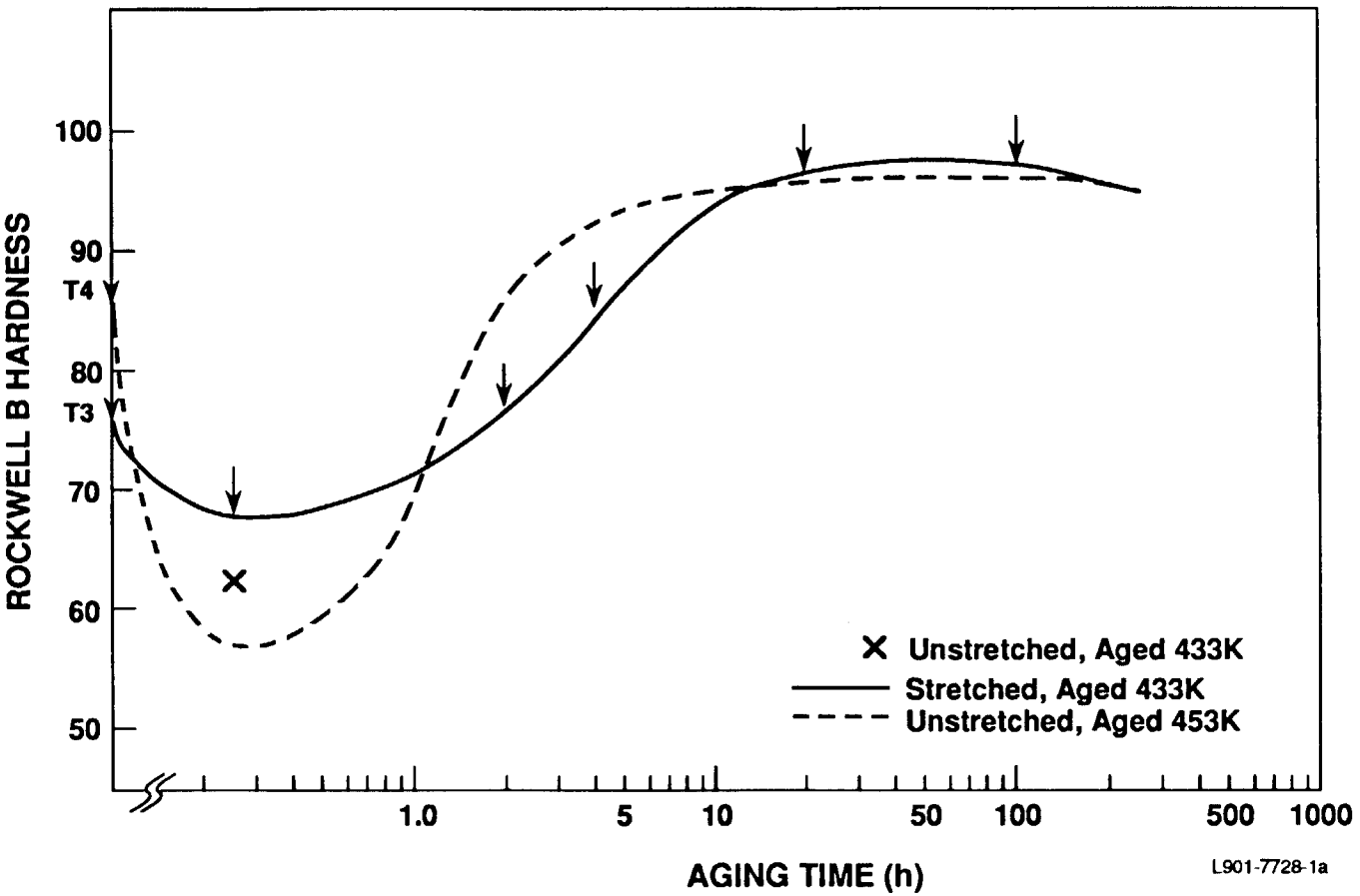

Figure1. Hardness variation with artificial aging time at 160°C (433K) for the stretched (T3) and at 180°C (453K) for the unstretched (T4) material.

The SAD patterns using a [110] zone axis for the T4 condition (Fig. 2a), and those after 15-min exposure to 160°C (433K) (Fig. 2b) or 180°C (453K) (Fig. 2c) show that a) the naturally aged microstructure consists of GP zones and θ', b) upon 15 min artificial aging at 160°C (433K), a significant amount of the δ' dissolves leaving a microstructure of some δ' and GP zones (Fig. 2b) in the aluminum solid solution, and c) 15 min artificial aging at the higher temperature of 180°C (453K) leaves a diffuse SAD pattern where <100> streaking due to the GP zones (Fig. 2c) can still be discerned.

Similarly, SAD patterns for the stretched material in the T3 condition and after aging for 15 minutes at 160°C (433K) and 180°C (453K) are compared in Figs. 3a-c. In the T3 condition (Fig. 3a), δ' (Al_3Li) spots are readily seen, although the GP zones, while present, are not as prominent as in the T4 condition (compare <100> streaking in Fig. 2a with Fig. 3a). Artificial aging at 160°C (433K) for 15 min results in the dissolution of GP zones and some δ'. In addition, θ' is possibly present as can be seen from the [100] zone axis SAD pattern in Fig. 3b. The strain and dislocation substructure introduced by the prior stretching operation make it difficult to obtain and interpret the diffraction patterns in this reverted condition. A [111] zone axis pattern of the material exposed to 180°C (453K) for 15 minutes (Fig. 3c) reveals the presence of T_1 precipitates, which suggests that this time at the higher temperature is sufficient to place the stretched material to the right of the reversion minimum on the aging curve (i.e., on the increasing hardness side). A hardness curve at this temperature for the T3 material is not shown in Fig. 1.

Microstructural evolution in the stretched material aged at 160°C (433K) for times longer than 15 min (i.e., to the right of the reversion minimum in Fig. 1) was followed on the transmission electron microscope using SAD (Figs. 4a-e). After 2 h at 160°C (433K), a [110] zone axis SAD pattern (Fig. 4a) reveals the presence of all four variants of the T_1 phase and in addition, <100> streaking typical of the θ' phase. The maximum in intensity at the mid point of the <100> streaks derives from θ' but is also coincident with a δ' superlattice reflection. In this case, the elliptical shape of this intensity maximum leads to the belief that this is a consequence of the θ' phase and not δ'.

A [100] zone axis SAD pattern (Fig. 4b) of the material exposed to 160°C (433K) for 4h reveals the presence of θ' in the form of <100>

Figure 2 SAD patterns of the unstretched material using a [110] zone axis for a) the T4, b) T4 + 15 min at 160°C (433K), and c) T4 + 15 min at 180°C (453K) conditions.

Figure 3. SAD patterns of the stretched material using a) [110] zone axis for the T3, b) [100] zone axis for the T3 + 160°C (433K), and c) [111] zone axis for the T3 + 180°C (453K) conditions.

(a)

(b)

(c)

Figure 4(a),(b),(c) SAD patterns of the stretched material using a) [110] zone axis for the T3 + 2 h, b) [100] zone axis for the T3 + 4 h, c) [112] zone axis for the T3 + 4 h.
(Figure 4 continued on next page)

(e)

(d)

Figure 4(d),(e) SAD patterns of the stretched material using d) [110] zone axis for the T3 + 20 h, and e) [110] zone axis for the T3 + 102 h, at 160°C (433K).

streaks that intersect and give rise to a maximum in intensity that coincides with the superlattice reflection that would arise from δ'. However, the observed intensity is attributed to θ', again because of the shape of the bright spot, which appears as an intersection of two ellipses rather than a circular spot which is characteristic of the δ' phase. In addition to the θ' phase, symmetrically distributed around the <100> intersection maximum are the four spots corresponding to the T_1 variants. A [112] zone axis SAD pattern (Fig. 4c) of the 4 h specimen confirms the existence of the T_1 phase and also reveals faint streaking in the <210> directions. This family of streaks is attributed to the Al_2CuMg S' phase. Thus, after 4 h at 160°C (433K), the stretched material contains θ', T_1, and the S' phase. It must be specified that structure factor modifications due to compositional changes within the precipitate phases can account for modified diffraction spot intensities and work is currently in progress to measure the compositions of the individual phases.

Moving further up the aging curve, in the slightly underaged condition that corresponds to 20 h at 160°C (433K), an SAD pattern based on a [110] zone axis (Fig. 4d) reveals the presence of T_1 and θ'. The [112] zone axis SAD pattern confirms the presence of the S' phase.

In the overaged condition corresponding to a 102 h at 160°C (433K) (Fig. 4e), the T_1 phase is the only major strengthening phase present; the presence of <100> streaks corresponding to the θ' phase in this condition could not be reliably confirmed and, if present, is in only small amounts. Similarly, the <210> streaks due to the S' phase were not reliably confirmed.

A bright-field and a corresponding T_1 dark field micrograph in the slightly underaged condition of 20 h at 160°C (433K) are shown in Figs. 5a and 5b, respectively. Even in this near peak-aged condition, the T_1 precipitates are extremely fine and homogeneously distributed.

4. DISCUSSION

The observed higher hardness in the T4 condition compared to the T3 condition is attributed to the greater amount of GP zones in the former, although fine θ' and GP zones are present in both the T3 and T4 conditions. Likewise, the large drop in hardness upon reverting the T4 material at 180°C (453K) is associated with the dissolution of θ' and

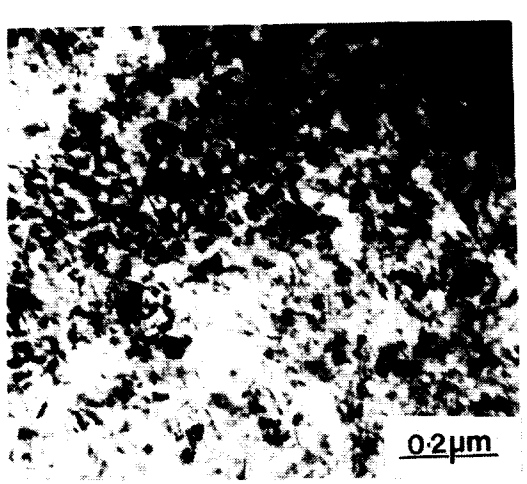

(a)

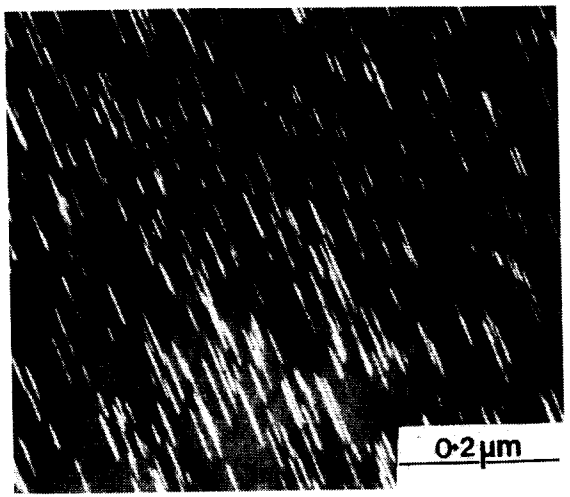

(b)

Figure 5 Typical microstructure in the near-peak-aged condition of T3 + 20 h at 160°C (433K) in a) bright field and b) T_I dark field.

some of the GP zones. The decrease in hardness for this material is not as dramatic when reversion is performed at 160°C (433K), where more GP zones are still present. A direct comparison of the reverted T4 with the reverted T3 material (433K) reveals that the hardness of the latter is higher. The exact reasons for this difference are unclear but must arise from a complicated interplay of the work-hardening residual from the stretch, δ' and what appears to be θ' precipitates.

In the underaged condition of 2 h at 160°C (433K), the stretched material contains the T_1 and θ' phases, which is in agreement with the recent work of Gayle et al. (4) on the unstretched material. However, they also found the S' phase (4) which, in this study, was observed after 4 h of aging the T3 specimens. In addition, Gayle et al. (4) provide evidence of a new phase, denoted ν, but we made no effort to locate it in this study. After 20 h at 160°C (433K), T_1, θ' and S' were present, whereas Langan and Pickens (2) observed only the T_1 phase in a similar alloy after 24 h at 160°C (433K). However, over-aging the stretched material in the present study at 160°C (433K) for 102 h causes the dissolution of both θ' and a significant amount of the S' phases leading to a microstructure which is predominantly strengthened by the T_1 phase dispersed in an a solid solution. Perhaps a significant amount of the θ' and S' dissolved after 24 h as observed earlier (2), even though they are present after 20 h at 160°C (433K) in this study.

The observed high strengths in these alloys in the naturally aged conditions (T3 and T4), are attributed to a combination of the fine δ' and GP zones. In the artificially aged conditions (T6 and T8) high strength is primarily a result of the extremely fine T_1 precipitates homogeneously distributed throughout the matrix.

Lithium, magnesium, and zirconium exhibit very high solute-vacancy binding energies in aluminum (7-9). Consequently, vacancies present at the solutionizing temperature are retained during quenching rather than migrating to sinks such as grain boundaries. For the specific case of binary Al-Li alloys, Suzuki et al. (10) suggest that excess vacancies bound to lithium atoms are confined to the δ' phase during aging. Excess vacancies may contribute to the precipitation process in Weldalite 049-type alloys by two mechanisms. First, when the δ' present during natural aging dissolves during reversion, the released vacancies may act as nucleation sites for the plate-like T_1 phase. Second, vacancies that were bound to Mg and Zr, as well as

released vacancies that are now likely bound to Li atoms, are unavailable to assist lattice diffusion, thereby retarding growth of T_1. Consequently, the vacancies are effectively utilized for enhancing nucleation and discouraging growth, which is consistent with the fine distribution of T_1 observed even in the overaged condition. The effects of such trace elemental additions on precipitation have been demonstrated previously (11, 12) in other aluminum alloys. In addition, the role of these trace elements such as Ag and Mg in influencing precipitate-matrix interfacial energies and/or the possibility of these elements segregating to the interface and acting as diffusional barriers cannot be ignored as both these factors can significantly affect precipitation kinetics.

Prior to significant δ' precipitation after quenching, the stretching operation introduces a significant number of dislocations which may act as vacancy sinks by sweeping vacancies away, thereby decreasing the vacancy concentration available for influencing the natural aging response. However, dislocations are also effective nucleation sites of the T_1 precipitates. That is, in the stretched material, heterogeneous nucleation on dislocations likely occurs in addition to the somewhat reduced nucleation frequency at vacancies in a way that approximately equals the nucleation at vacancies in the unstretched material.

5. CONCLUSIONS

The microstructural evolution during artificial aging of an Al-Cu-Li-Ag-Mg-Zr alloy has been characterized using TEM both with and without prior cold work. In the stretched and near-peak aged condition, a fine homogeneous distribution of T_1, θ' and S' phases is present in an a solid solution matrix, but on over-aging, virtually all of the θ' and most of the S' dissolve leaving behind a microstructure of essentially T_1 precipitates in an a aluminum solid solution matrix. It is suggested that trapped-in excess vacancies play a significant role in refining the microstructure by enhancing precipitate nucleation and discouraging their growth.

7. REFERENCES

[1] J.R. Pickens, F.H. Heubaum, T.J. Langan, and L.S. Kramer, in "Aluminum-Lithium Alloys" (Proceedings of the Fifth International Aluminum-Lithium Conference), T.H. Sanders and E.A. Starke, eds., MCE Publications Ltd., Birmingham, U.K., 1989, p. 1397.

[2] T.J. Langan and J.R. Pickens, ibid., p. 691.

[3] F.W. Gayle, F.H. Heubaum, and J.R. Pickens, op. cit., p. 701.

[4] F.W. Gayle, F.H. Heubaum, and J.R. Pickens, Scripta Metall., 24, 1990, p. 79.

[5] R.J. Rioja, P.E. Bretz, R.R. Sawtell, W.H. Hunt, and E.A. Ludwiczak, in "Aluminum Alloys, Their Physical and Mechanical Properties," Vol. III, Proceedings of the International Conference on Aluminum Alloys, Chameleon Press, London,U.K., 1986, p. 1781.

[6] W.A. Cassada, G.J. Shiflet, and E.A. Starke, Jr., J. de Physique, colloq. C3, Vol. 48, 1987, p. 397.

[7] M. Ahmad and T. Ericsson, Scripta Metall., 19, 1985, p. 457.

[8] S. Ozbilen and H.M. Flower, Acta Metall., 37, 1989, p. 2993.

[9] S. Ceresara, A. Giarada, and A. Sanchez, Philos. Mag., 35, 1977, p. 97.

[10] H. Suzuki, M. Kanno, and N. Hayashi, J. Jpn. Inst. Light Metals, 31, 1981, p. 122.

[11] B.C. Muddle and I.J. Polmear, Acta Metall., 37, 1989, p. 777.

[12] W.X. Feng, F.S. Lin, and E.A. Starke, Jr., Metall. Trans. A, 15, 1984, p. 1209.